Calculation of magnetic x-ray dichroism in 4*d* and 5*d* absorption spectra of actinides

H. Ogasawara and A. Kotani*
Department of Physics, Faculty of Science, Tohoku University, Sendai 980, Japan

B. T. Thole
Department of Chemical Physics, University of Groningen, Nijenborgh 16, 9747 AG Groningen, The Netherlands
(Received 9 November 1990; revised manuscript received 6 March 1991)

We present atomic calculations of the magnetic dichroism in 4*d* and 5*d* x-ray-absorption (XAS) spectra of trivalent actinide ions. The calculations are carried out for both linearly and circularly polarized light at zero temperature. Large magnetic dichroism is predicted for 5*d* XAS with polarization-dependent spectral shape and intensity. For 4*d* XAS the spectral shape is less polarization dependent, but the branching ratio is expected to be very sensitive to solid-state effects.

I. INTRODUCTION

Actinide elements have a partially filled 5*f* shell, which in solids becomes localized like the 4*f* shell of rare earth or itinerant like the 3*d* shell of transition metals depending on the circumstances. They have attracted much interest due to this intermediate nature of the 5*f* electrons. High-energy spectroscopy can be a useful probe to investigate the properties of those 5*f* electrons, as was already shown in rare-earth and transition-metal compounds.[1] There have been, however, few experiments, except for Th and U compounds, because they are very rare, some of them only occur as co-products of atomic reactions and their radiation requires special facilities.

In this paper we calculate 4*d* ($N_{4,5}$) and 5*d* ($O_{4,5}$) x-ray absorption spectra (XAS) of trivalent actinide ions (except for Th^{4+}) placed in a magnetic field for nonpolarized, linearly and circularly polarized light. We consider the localized limit, where actinide 5*f* states are treated as localized ionic moments. The effects of the solid state such as crystal field or mixing with ligand bands are neglected. This approximation worked quite well for describing rare-earth metals 3*d* ($M_{4,5}$) and 4*d* ($N_{4,5}$) XAS,[2,3] which have fine multiplet structures due to the interaction between the 4*f* electrons and the core hole created by the photon and the selection rules of dipole transition. For some actinide systems, we expect that this approach still works well, while for many actinide compounds, this approach can only serve as a starting point to assess the possibilities of XAS.

Magnetic x-ray dichroism (MXD) is a recently developing technique attracting attention as a new probe for the local electronic states of magnetic systems. It can give information on the orientation and size of local magnetic moments, which is complementary to other techniques giving global information. It has already been shown that large MXD effects exist in 3*d* XAS of rare-earth elements with linearly polarized x rays both theoretically and experimentally.[4–7] MXD is also observed in Fe 1*s*, Gd 2*p*, and Tb 2*p* XAS.[8,9] Theoretical calculations of 3*d* and 4*d* XAS in rare earths with circularly polarized light predict large MXD.[10–12]

Polarized x rays are difficult to generate by procedures usually used for optical light. Synchrotron radiation enables us to obtain both linearly and circularly polarized light over wide frequency ranges including the x-ray region. Linearly polarized x rays are already available in many storage rings. Circularly polarized x rays are also available using out-of-plane radiation, but this is not very effective because the intensity becomes rather low compared to the on-plane linearly polarized light. Recently special insertion devices to obtain high-intensity circularly polarized x rays have become available. With these circumstances in mind, it is expected that MXD measurements with both linearly and circularly polarized light will be made for some actinides systems in the near future, though there have been no experiments so far.

The organization of this paper is as follows. In Sec. II we present the calculated results of unpolarized 4*d* and 5*d* XAS spectra for a series of actinide ions. The branching ratio of 4*d* XAS is discussed from *JJ* and *LS* coupling schemes. In Sec. III we show the MXD of 4*d* and 5*d* XAS spectra both for linearly and circularly polarized light. Some discussions on characteristic features of the calculated MXD are given in Sec. IV. Section V is devoted to the conclusion.

II. UNPOLARIZED 4*d* AND 5*d* XAS OF ACTINIDES

The 4*d*, 5*d*, and 5*f* shells of actinide (Ac) elements have the same general characteristics as 3*d*, 4*d*, and 4*f* shells of rare-earth (RE) elements, respectively. The excitation energy ranges near 1000 eV in 4*d*(Ac) and 3*d*(RE) XAS or near 100 eV in 5*d*(Ac) and 4*d*(RE) XAS. 3*d*(RE) or 4*d*(Ac) XAS are split into $d_{5/2}$ and $d_{3/2}$ components by the large core hole spin-orbit interaction, and each component has extra structures due to electron-electron interaction. 4*d*(RE) or 5*d*(Ac) XAS do not show obvious spin-orbit splitting, because the electron-electron interaction between core hole and *f* electron is much larger than the spin-orbit interactions (so the final states are expressed rather in *LS* coupling). Their spectrum is divided into a prethreshold region and a giant absorption region. The prethreshold region lies near (or below) threshold,

being pushed down by exchange interaction. It consists of dipole forbidden states and shows weak fine structures. The giant absorption region consists of dipole allowed states and has large intensity and broad structures high above the threshold.

Published experiments of $4d$ and $5d$ XAS of actinide materials are rare. We could only find those of Th and U metals[13–15] and some of their compounds. The experimental $4d$ XAS spectra of Th and α-U are similar to those of their lanthanide counterparts La and Nd.[16] But α-U $4d$ XAS shows small extra structures on the $4d_{5/2}$ and $4d_{3/2}$ components. The Th $5d$ XAS is almost the same as the La $4d$ XAS, whereas the prethreshold region of α-U $5d$ XAS is much stronger and broader than that of Nd $4d$ XAS.

We calculate $4d$ and $5d$ XAS for free actinide ions. Although actinide ions in solids can take on different valences depending on the circumstances, we only treat the trivalent ones except for Th^{4+}. The spectrum of an other valence state can be obtained approximately from a neighboring atom with the same f count. The ground state of $5f^n|\alpha JM\rangle$ cannot always be well approximated by LS coupling because LS states are mixed strongly by spin-orbit interaction. For Am, for instance, the Hund's-rule LS state contributes less than half to the ground state. Still the J value predicted by Hund's rule is correct. The final states $d^9 5f^{n+1}|\alpha' J' M'\rangle$ are those which can be reached from the ground state under the dipole selection rules $\Delta J = 0, \pm 1$ ($J = J' = 0$ is excluded). Transitions to np continuum states are ignored. The values of parameters such as Slater integrals and spin-orbit coupling constants are obtained by Cowan's atomic Hartree-Fock (HF) program with relativistic corrections.[17] This calculation is done for the average of the configuration both for $5f^n$ and $d^9 5f^{n+1}$. The Coulomb and exchange integrals $F^k(5f,5f)$, $F^k(4d,5f)$, $G^k(4d,5f)$, $F^k(5d,5f)$, and $G^k(5d,5f)$ are reduced to 80%, 80%, 80%, 75%, 66% of their HF values, respectively. These reduction rates are appropriate for lanthanides.[2,3] The reduced values are given in Table I–III.

Calculated results of unpolarized $4d$ XAS and $5d$ XAS are shown in the top panel of Figs. 1 and 2, respectively, where the origin of the incident photon energy ω is taken arbitrarily. The calculations are done with Cowan's program,[17] and the plotted curve is a Lorentzian convolution of the line spectra. The broadening widths Γ (half width at half maximum) are also given in Tables I and II. The widths of $4d_{5/2}$ and $4d_{3/2}$ are taken to be equal for simplicity. Actually, the $4d_{3/2}$ component is expected to be broader, because there is an additional Coster-Kronig decay channel, and it will also show an asymmetric Fano shape due to the overlap with the continuum.[2] In the $5d$ XAS, the widths for prethreshold and giant absorption regions are quite different when the number of f electrons is small, as found experimentally for the metals Th and α-U. Therefore, we take a smaller spectral width Γ for the prethreshold region of Th, Pa, and U. The calculated results for tetravalent Th and trivalent U free ions seem to agree with the experiments for Th and α-U metals, respectively. After Np, however, the prethreshold region and the giant region overlap in the calculated spectra, and the boundary between them is not clear. Therefore, the convolution of the spectra is made only with the Γ for the giant absorption region.

A special feature of $4d$ XAS in actinides is the high value of the $d_{5/2}$:$d_{3/2}$ branching ratio. Note the different intensity scale for $d_{5/2}$ and $d_{3/2}$ components in Fig. 1. The origin of the high branching ratio is the large $5f$ spin-orbit coupling in the ground state. This mixes other LS terms into the Hund's-rule ground term, increasing the expectation value of the angular part of the spin-orbit coupling and thereby increasing the branching ratio.[18] In the Hund's-rule term the spins and orbits are first coupled to a total L and S and these are coupled to a total J, which yields a moderate average coupling of each individual spin with its orbit. But when the spin-orbit interaction increases each spin couples directly to its orbit yielding a much higher spin-orbit expectation value (at the expense of exchange and Coulomb energy). Of course this extra effect is absent when there is only one electron or hole and it is most important near the middle of the series.

In order to show the importance of the $5f$ spin-orbit interaction in $4d$ XAS of actinides, we calculate the branching ratio taking into account only the spin-orbit interaction (i.e., disregarding all electron-electron interac-

TABLE I. Parameter values for initial states.

Z		n	J	$F^2_{(5f,5f)}$	$F^4_{(5f,5f)}$	$F^6_{(5f,5f)}$	ζ_{5f}
90	Th^{4+}	0	0.0				
91	Pa^{3+}	2	4.0	6.71	4.34	3.17	0.202
92	U^{3+}	3	4.5	7.09	4.60	3.36	0.235
93	Np^{3+}	4	4.0	7.43	4.83	3.53	0.270
94	Pu^{3+}	5	2.5	7.76	5.05	3.70	0.307
95	Am^{3+}	6	0.0	8.07	5.26	3.86	0.345
96	Cm^{3+}	7	3.5	8.37	5.46	4.01	0.386
97	Bk^{3+}	8	6.0	8.65	5.65	4.15	0.428
98	Cf^{3+}	9	7.5	8.93	5.84	4.29	0.473
99	Es^{3+}	10	8.0	9.19	6.02	4.42	0.520
100	Fm^{3+}	11	7.5	9.45	6.19	4.55	0.569
101	Md^{3+}	12	6.0	9.71	6.36	4.68	0.620
102	No^{3+}	13					0.674

TABLE II. Parameter values for 4*d* XAS final states.

Z		$F^2_{(5f,5f)}$	$F^4_{(5f,5f)}$	$F^6_{(5f,5f)}$	ζ_{5f}	ζ_{4d}	$F^2_{(4d,5f)}$	$F^4_{(4d,5f)}$	$G^1_{(4d,5f)}$	$G^3_{(4d,5f)}$	$G^5_{(4d,5f)}$	Γ
90	Th^{4+}				0.181	12.3	3.54	1.39	0.63	0.67	0.56	1.0
91	Pa^{3+}	7.16	4.66	3.41	0.235	16.4	3.50	1.38	0.61	0.65	0.55	1.0
92	U^{3+}	7.50	4.88	3.57	0.269	17.4	3.77	1.50	0.65	0.70	0.59	1.0
93	Np^{3+}	7.82	5.10	3.74	0.305	18.5	4.02	1.61	0.69	0.75	0.64	1.0
94	Pu^{3+}	8.12	5.30	3.89	0.342	19.6	4.26	1.72	0.73	0.80	0.68	1.0
95	Am^{3+}	8.41	5.50	4.04	0.382	20.8	4.50	1.83	0.77	0.84	0.72	1.0
96	Cm^{3+}	8.70	5.69	4.18	0.423	22.0	4.72	1.93	0.80	0.88	0.75	1.0
97	Bk^{3+}	8.97	5.87	4.32	0.467	23.3	4.94	2.04	0.84	0.92	0.79	1.0
98	Cf^{3+}	9.23	6.05	4.45	0.513	24.7	5.16	2.14	0.87	0.97	0.83	1.0
99	Es^{3+}	9.49	6.22	4.58	0.560	26.1	5.37	2.23	0.90	1.01	0.86	1.0
100	Fm^{3+}	9.74	6.39	4.70	0.611	27.6	5.57	2.33	0.93	1.05	0.90	1.0
101	Md^{3+}				0.664	29.1	5.78	2.43	0.97	1.09	0.93	1.0
102	No^{3+}					30.7						1.0

TABLE III. Parameter values for 5*d* XAS final states. The Γ values in parenthesis for Th, Pa, and U are used for prethreshold region.

Z		$F^2_{(5f,5f)}$	$F^4_{(5f,5f)}$	$F^6_{(5f,5f)}$	ζ_{5f}	ζ_{5d}	$F^2_{(5d,5f)}$	$F^4_{(5d,5f)}$	$G^1_{(5d,5f)}$	$G^3_{(5d,5f)}$	$G^5_{(5d,5f)}$	Γ
90	Th^{4+}				0.208	2.70	7.28	4.64	7.43	4.59	3.27	2.0(0.2)
91	Pa^{3+}	6.94	4.51	3.30	0.216	2.92	7.19	4.56	7.32	4.51	3.21	2.0(0.5)
92	U^{3+}	7.29	4.74	3.47	0.249	3.17	7.57	4.83	7.78	4.80	3.41	2.0(0.5)
93	Np^{3+}	7.61	4.96	3.64	0.284	3.44	7.93	5.08	8.20	5.06	3.61	2.0
94	Pu^{3+}	7.92	5.17	3.79	0.321	3.71	8.26	5.31	8.60	5.31	3.79	2.0
95	Am^{3+}	8.22	5.37	3.94	0.359	4.00	8.58	5.53	8.98	5.55	3.96	2.0
96	Cm^{3+}	8.50	5.56	4.08	0.399	4.31	8.88	5.74	9.34	5.78	4.13	2.0
97	Bk^{3+}	8.78	5.74	4.22	0.441	4.62	9.17	5.95	9.68	6.00	4.29	2.0
98	Cf^{3+}	9.04	5.92	4.35	0.486	4.96	9.45	6.15	10.01	6.21	4.44	2.0
99	Es^{3+}	9.30	6.09	4.48	0.533	5.31	9.73	6.34	10.33	6.41	4.58	2.0
100	Fm^{3+}	9.56	6.26	4.61	0.582	5.67	10.0	6.52	10.65	6.61	4.73	2.0
101	Md^{3+}				0.634	6.05	10.26	6.70	11.0	6.80	4.87	2.0
102	No^{3+}					6.45						2.0

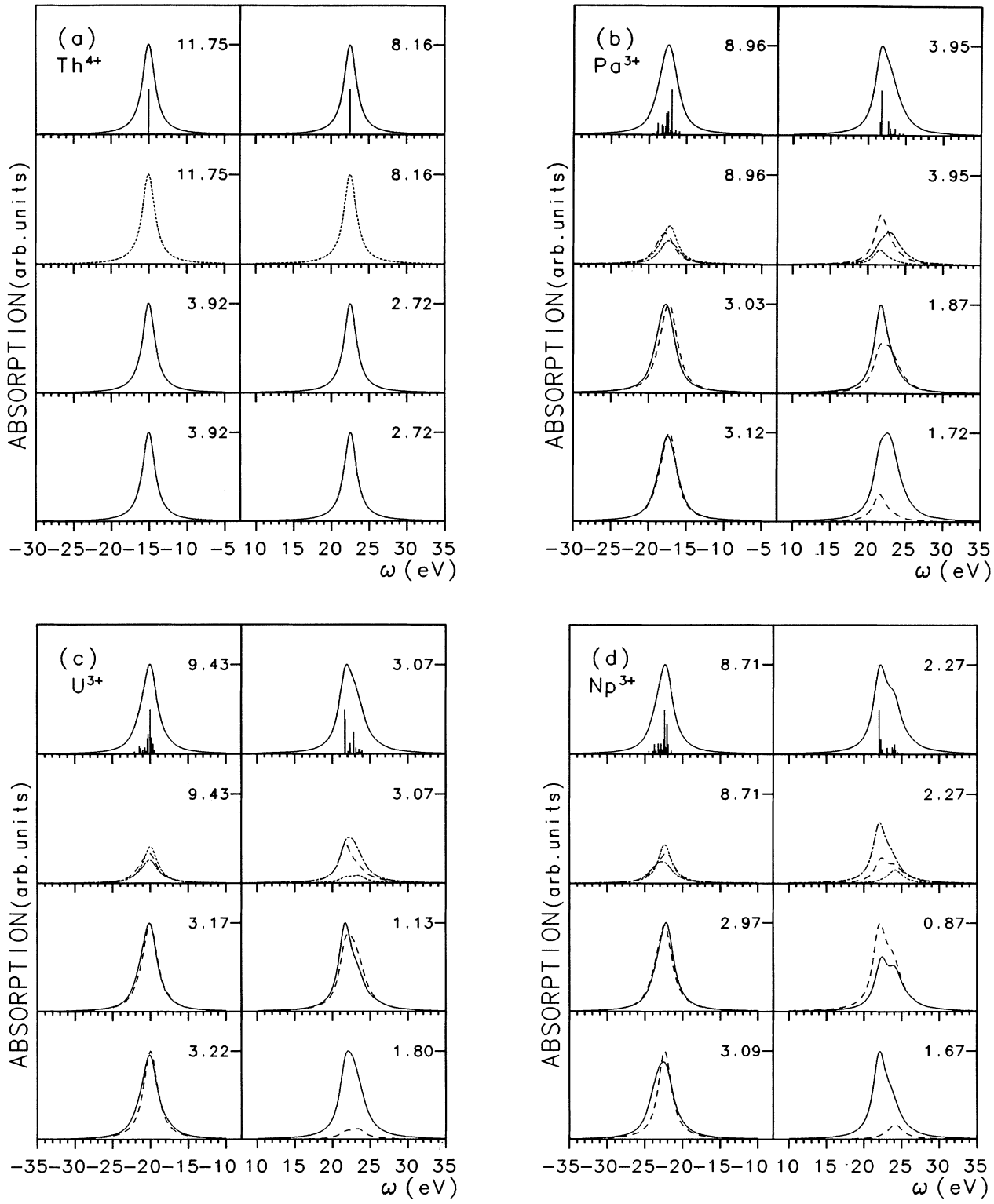

FIG. 1. The top panels: calculated $4d \rightarrow 5f$ x-ray absorption spectra of trivalent actinide ions (except for Th^{4+}). The curves are a Lorentzian convolution of the line strength plotted as vertical bars in arbitrary scale. The right sides correspond to $4d_{3/2}$ components and the left sides to $4d_{5/2}$. The second panels: the same curves, on the same scale, for each ΔJ final state. The dotted curves correspond to $\Delta J = +1$, the dashed to $\Delta J = 0$, and the dash-dotted to $\Delta J = -1$. The third panels: MXD spectra for linearly polarized light at $T = 0$ K, $LP\|$ (solid lines) and $LP\perp$ (dashed curve). The bottom panels: MXD spectra for circularly polarized light at $T = 0$ K, RCP (solid curves) and LSP (dashed curves). Horizontal scale is excitation energy in eV. The origin is taken to be arbitrary.

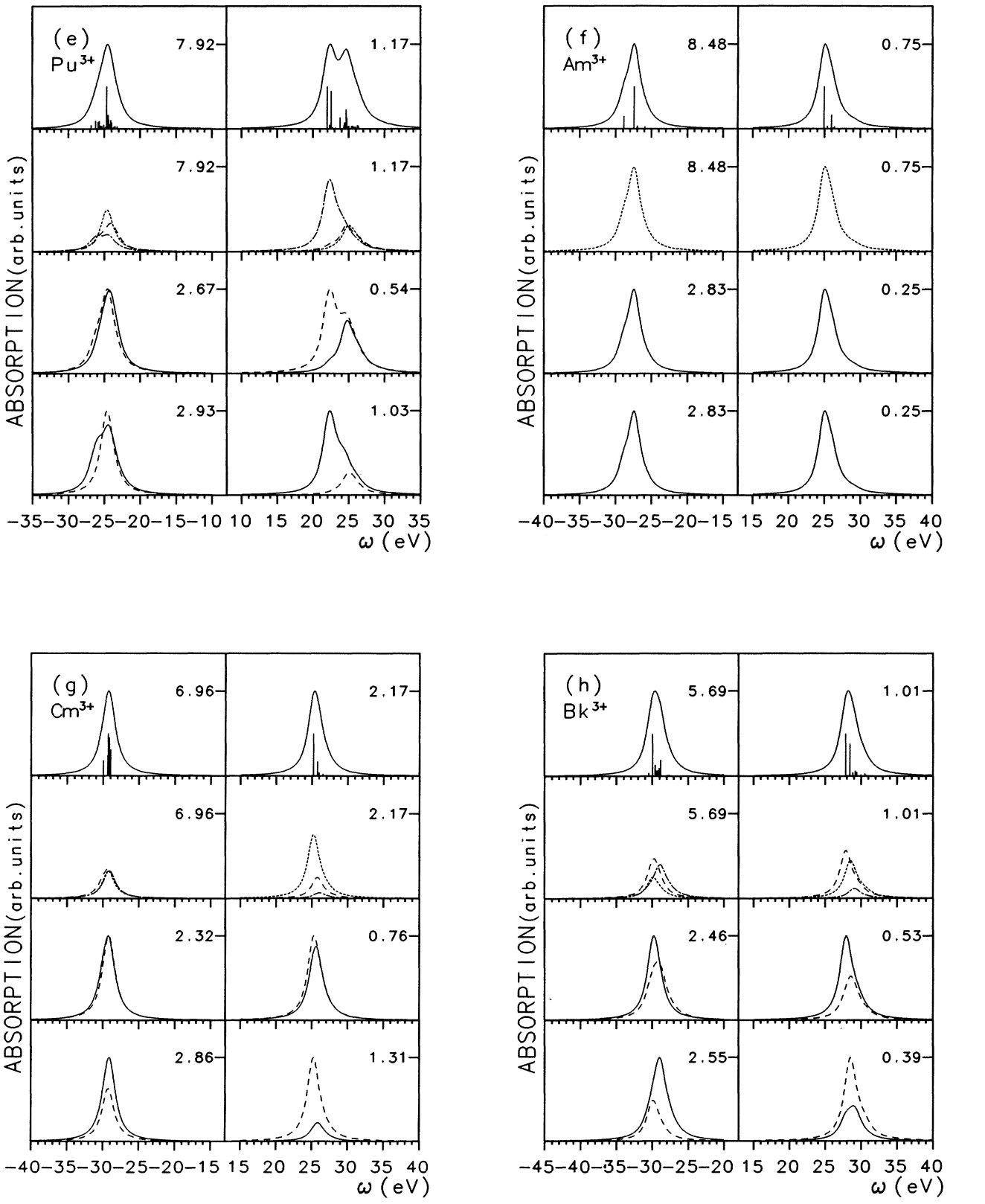

FIG. 1. (*Continued*).

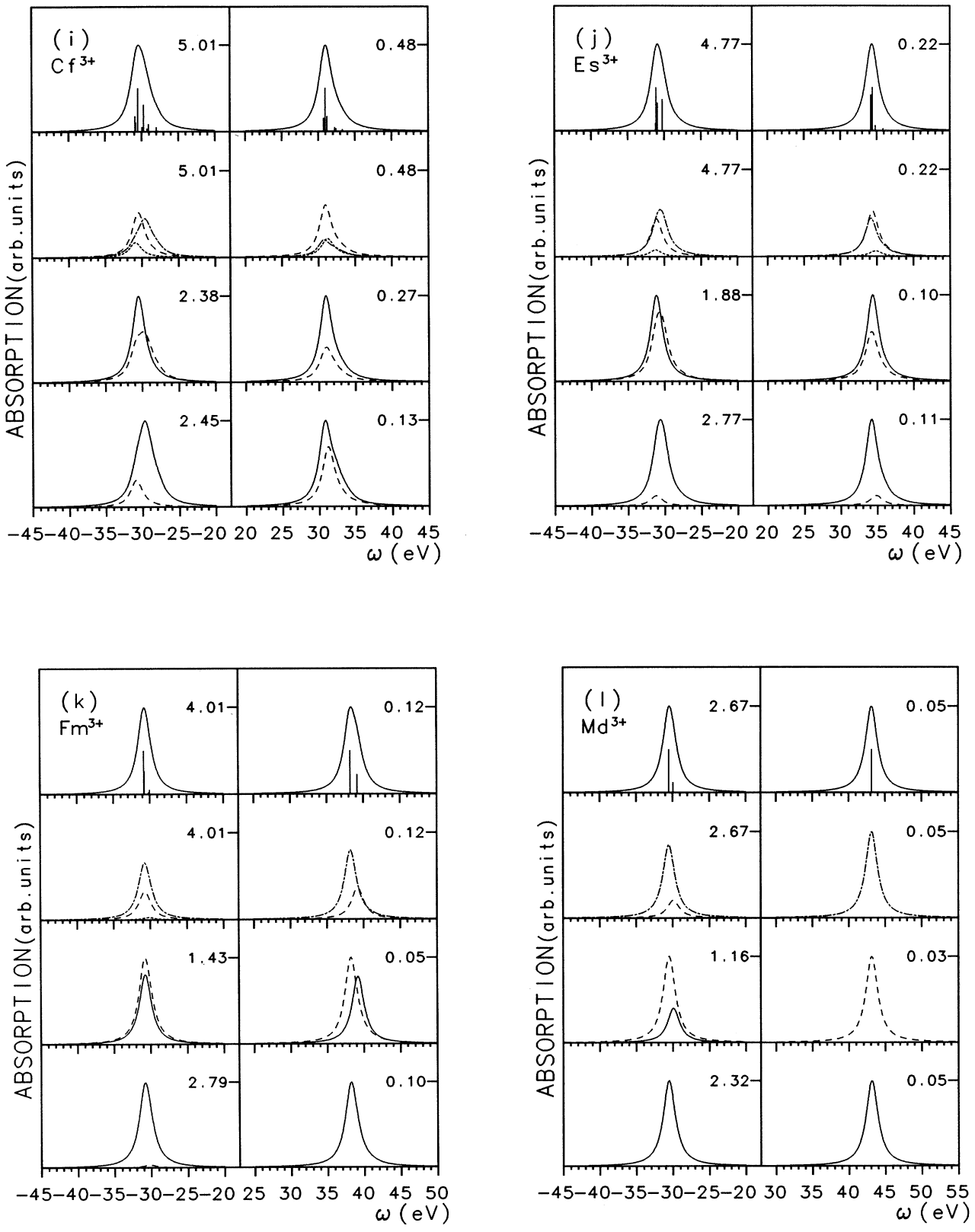

FIG. 1. (*Continued*).

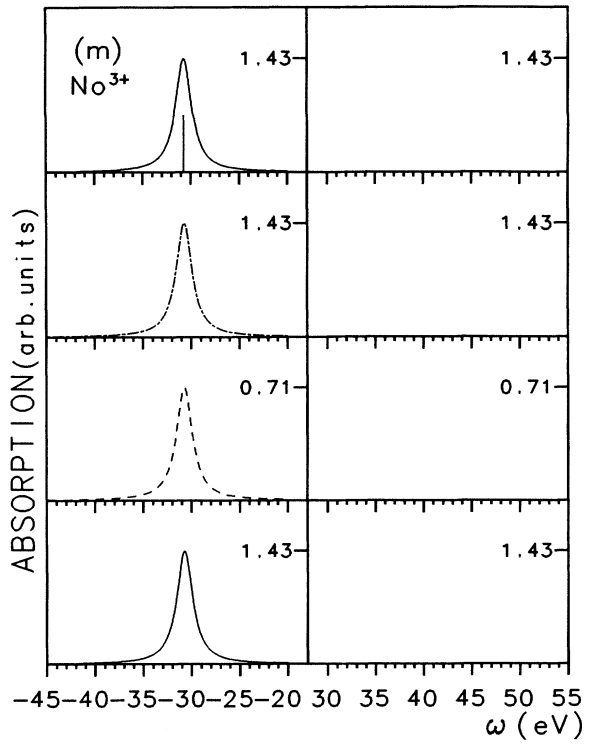

FIG. 1. (*Continued*).

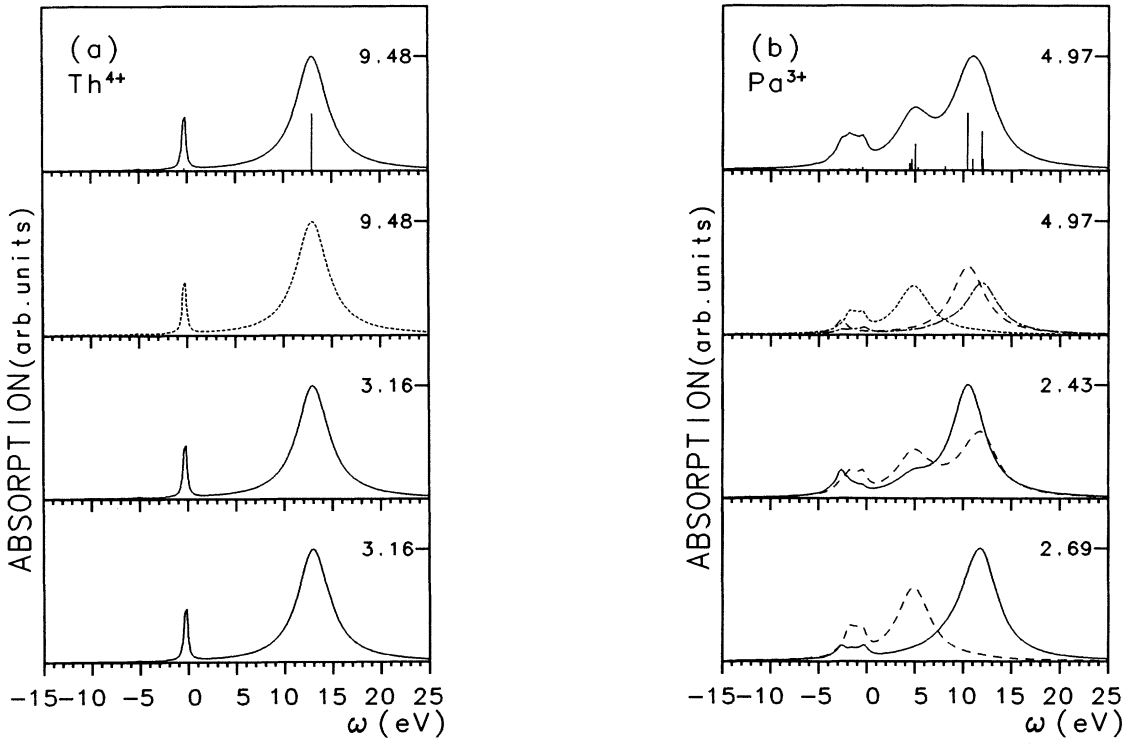

FIG. 2. The top panels: calculated $5d \rightarrow 5f$ x-ray absorption spectra of trivalent actinide ions (except for Th^{4+}). The curves are a Lorentzian convolution of the line strength plotted as vertical bars in arbitrary scale. Two different Lorentzian broadenings Γ for prethreshold and giant absorption regions are taken in Th, Pa, and U. The second panels: the same curves, on the same scale, for each ΔJ final state. The dotted curves correspond to $\Delta J = +1$, the dashed to $\Delta J = 0$, and the dash-dotted to $\Delta J = -1$. The third panels: MXD spectra for linearly polarized light at $T = 0$ K, $LP\|$ (solid curves) and $LP\perp$ (dashed curve). The bottom panels: MXD spectra for circularly polarized light at $T = 0$ K, RCP (solid curves) and LCP (dashed curves). Horizontal scale is excitation energy in eV. The origin is taken to be arbitrary.

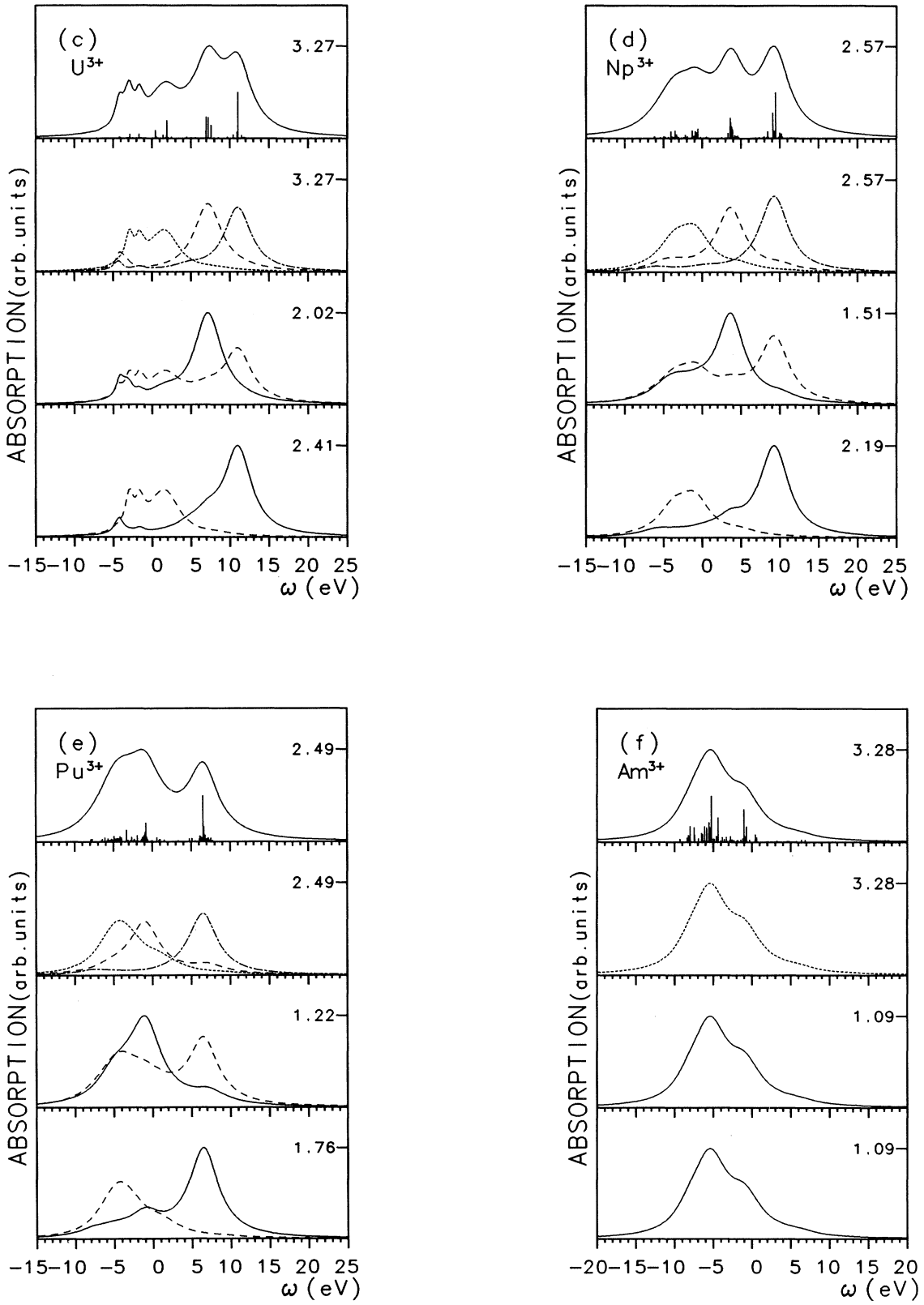

FIG. 2. (*Continued*).

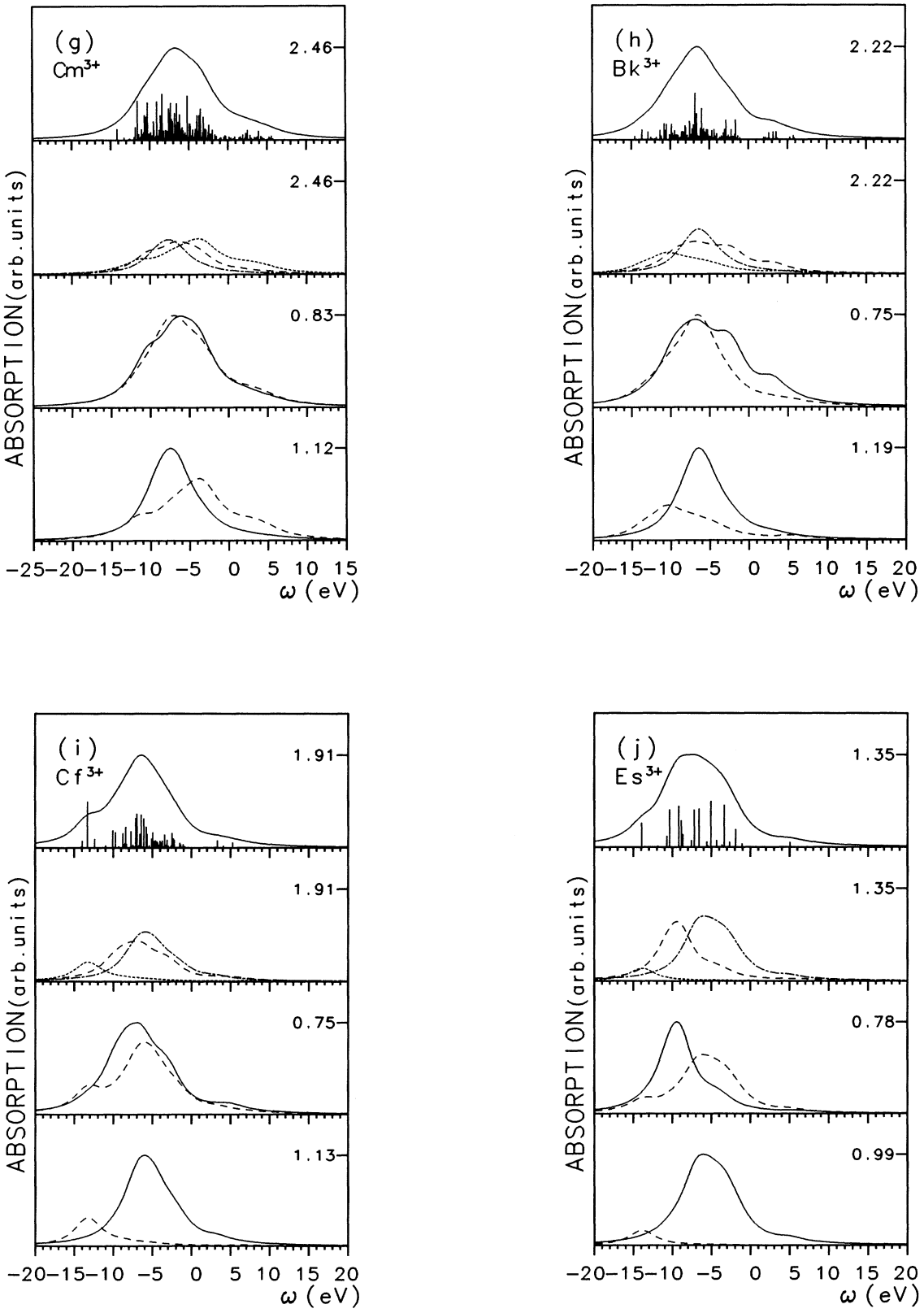

FIG. 2. (*Continued*).

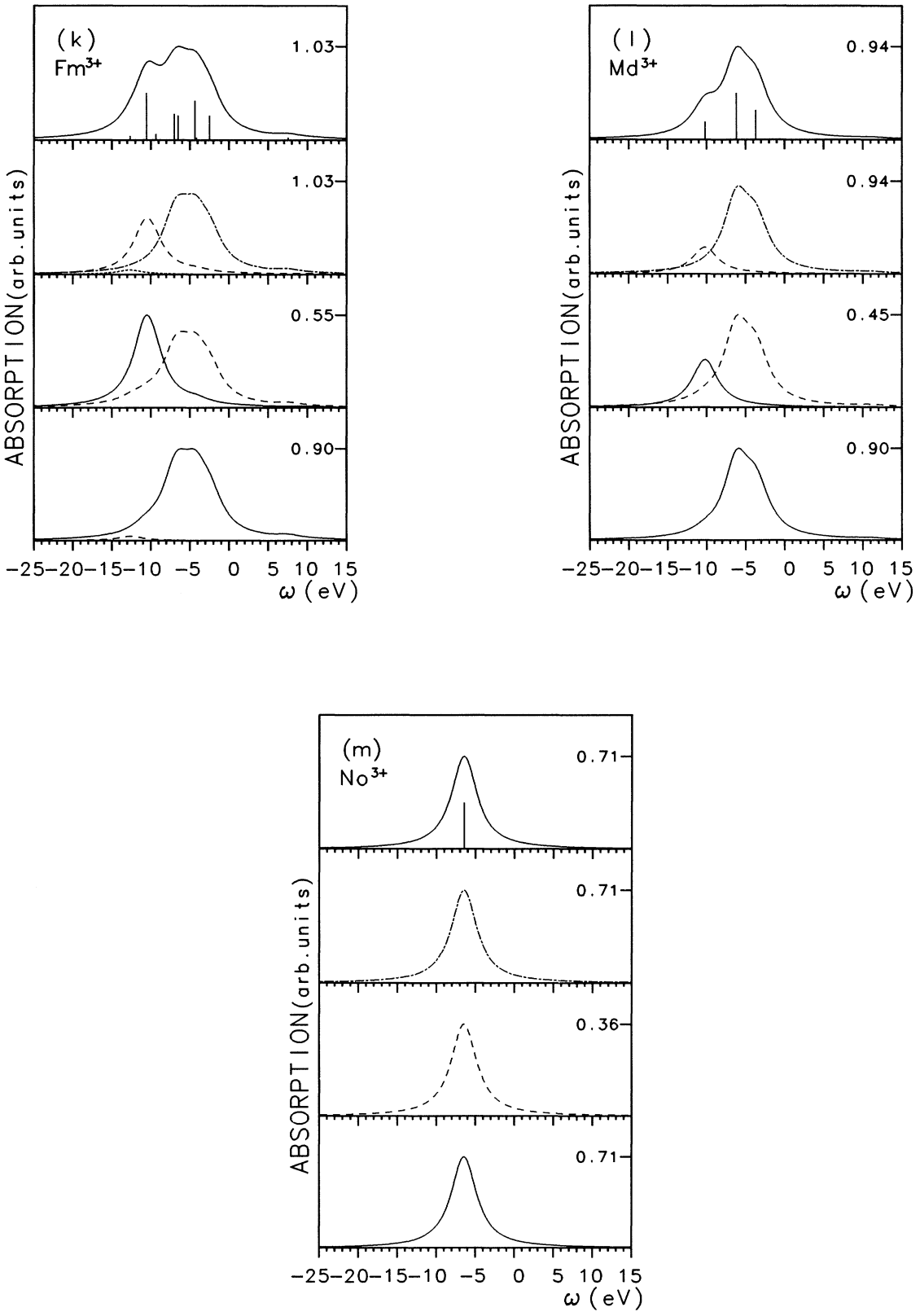

FIG. 2. (*Continued*).

TABLE IV. Branching ratio $I_{5/2}/(I_{5/2}+I_{3/2})]100$ of $4d$ XAS for LS and JJ limits and exact value. The exact value for $n=1$ is calculated, for completeness, with the parameter values for Pa^{3+}.

n	LS	JJ	Exact
0	60.0	60.0	59.2
1	64.1	64.1	63.4
2	66.7	68.9	68.0
3	68.5	74.5	72.3
4	69.3	81.3	76.0
5	68.9	89.6	81.7
6	66.7	100.0	91.8
7	60.0	100.0	75.2
8	66.7	100.0	84.9
9	73.3	100.0	92.2
10	80.0	100.0	95.9
11	86.7	100.0	96.6
12	93.3	100.0	98.1
13	100.0	100.0	100.0

tions). Observing that the expectation value of $l\cdot s$ of $f_{5/2}$ and $f_{7/2}$ electrons is -2 and $\frac{3}{2}$, respectively, the lowest spin-orbit energy (and the highest branching ratio) for $n\leq 6$ is obtained when all electrons are $\frac{5}{2}$, where n is the $5f$ electron number in the ground state. The branching ratio, $I_{5/2}/(I_{5/2}+I_{3/2})$, is then

$$B=\tfrac{3}{5}+8n/[15(14-n)]\ .$$

We obtain the same result when we calculate the average branching ratio of the holes, using for $\frac{5}{2}$ and $\frac{7}{2}$ holes a branching ratio of $\frac{1}{15}$ and 1, respectively. For $n\geq 6$ we get $B=1$ (all holes are $\frac{7}{2}$). This result (the JJ coupling limit) is shown in Table IV and compared with the exact branching ratio in the $4d$ XAS of actinides, as well as the branching ratio obtained in the LS coupling limit.[18] It is interesting to note that the JJ coupling limit is a better approximation than the LS limit. Only in f^7 the strong Coulomb interactions in ^8S resist the spin-orbit coupling appreciably. This suppression of spin-orbit coupling is also expected when crystal fields and hybridization are present, for which the $4d$ XAS should then be very sensitive.

III. MAGNETIC DICHROISM IN 4d AND 5d XAS SPECTRA

When a ground state f^n with total angular momentum J is placed in the presence of a magnetic field parallel to the z axis, it is split into $(2J+1)$ Zeeman components. Their energies are given by $-g\mu HM$, where g denotes Lande's g factor, μ the Bohr magneton, H the strength of magnetic field, and M the magnetic quantum number. If all Zeeman states are populated equally, practically no effect of the magnetic field will be observed, since the magnitude of magnetic splitting is of the order of 10 meV and the intrinsic line width due to the core hole lifetime is much larger. But if those levels are populated unequally according to the Boltzmann distribution, i.e., at low temperature and under high magnetic field, the spectral intensity will change with the polarity of the light, because the accessible final states are restricted also by selection rules for the magnetic quantum number [$m\equiv\Delta M=M'-M=0,\pm 1$ where $\Delta M=0$ is possible only if the light is parallel to the field and $\Delta M=+1(-1)$ only if the light is right (left) circularly polarized]. A detailed derivation is given in Ref. 6. In short, the three different sets of final states ($\Delta J=-1,0,+1$), displayed in the second panels of Figs. 1 and 2, are added not equally but with certain weighting factors $A^m_{JJ'}(\Theta)$ which depend on $J,\Delta J,m$, and reduced temperature $\Theta\equiv kT/g\mu H$. When $\Theta=0$, $A^m_{JJ'}(\Theta)$ takes a rather simple form as shown in Table V.[19]

TABLE V. The expression for the factors $A^m_{JJ'}(0)$.

	$m=0$	$m=\pm 1$
A^m_{JJ+1}	$\dfrac{2J+1}{(2J+3)(J+1)}$	$\dfrac{(J+1)(J+2)\mp(2J+3)+J^2}{2(2J+3)(J+1)}$
A^m_{JJ}	$\dfrac{J}{(J+1)}$	$\dfrac{J(J+1)\pm J-J^2}{2J(J+1)}$
A^m_{JJ-1}	0	$\dfrac{J(J-1)\pm J(2J-1)+J^2}{2J(2J-1)}$

We show the calculated results in the limit of $\Theta=0$ where only the lowest state ($M=-J$) is occupied and the largest dichroism is expected. The results for $4d$ XAS and $5d$ XAS are shown in Figs. 1 and 2, respectively. The third panel shows linear MXD spectra, where the full curve represents the polarization parallel to the magnetic field ($LP\|$) and the dashed one the perpendicular polarization ($LP\perp$). The bottom panel shows circular MXD spectra, where the full curve represents the right circular polarization (RCP) and the dashed one the left (LCP). Th and Am show no MXD because they have a $J=0$ ground state. Cm shows a bit different behavior to other $J\neq 0$ elements because of its $L=0$ ground state.

The spectral shape of $4d$ XAS does not show conspicuous polarization dependence for linearly nor circularly polarized light. The MXD is mostly seen on the polarization dependence of the spectral intensity. On the other hand, $5d$ XAS shows large MXD for both the intensity and the shape, especially in the giant absorption region. From the third panel it can be seen that two peaks appear for $LP\perp$ and a peak appears in the middle of these peaks for $LP\|$. From the bottom panel it can be seen that the peak for RCP appears on the high energy side of the one for LCP. The total intensity for RCP is larger than that for LCP. When the number of f electrons is larger than 8, the intensity for LCP decreases rapidly. These tendencies are more or less similar to those of lanthanide $4d$ XAS.

IV. DISCUSSION

Compared with the $3d$ XAS for lanthanides, $4d$ XAS spectra for actinides have rather simple structures for both the $d_{5/2}$ and $d_{3/2}$ components. This can be understood from Table II. In the final state of $4d$ XAS for ac-

tinides the spin-orbit coupling is much larger and the Slater integrals are smaller than those of $3d$ XAS for lanthanides; especially G^k for actinides is very small. Since the $4d$ and $5f$ orbits contain nodes, their overlap, and therefore the exchange integrals become small. This makes the energy difference between different ΔJ final states very small. That is why the spectra show little structure and the MXD only appears in the change of intensity. The branching ratio of the $d_{5/2}$ and $d_{3/2}$ components becomes much larger than that of $3d$ XAS for lanthanides because of the larger spin-orbit interaction of the $5f$ electrons.

The experiment shows that the $5d$ XAS in the prethreshold region for α-U is much stronger and broader than lanthanide $4d$ XAS for Nd which has the same number of f electrons. Since the prethreshold region mainly consists of dipole forbidden states, their intensity comes from a small admixture of dipole allowed states through the spin-orbit coupling in the final state. For α-U, the Slater integrals are smaller than those for Nd, while the spin-orbit coupling constant is about twice as large. Therefore the total intensity in the prethreshold region for α-U becomes much larger than for Nd. But it is not clear whether also the broadening is due to this effect or to some other ignored solid state effect or only to experimental resolution.

In order to discuss the behavior of MXD in more detail, we show the typical values of $A^m_{JJ'}(0)$ for each value of ΔJ and m in Table VI. The $A^m_{JJ'}(0)$ depend also on J, but the dependence is rather small; for instance, when J changes from $\frac{5}{2}$ to 8, $A^{-1}_{JJ+1}(0)$ changes from 0.75 to 0.89. From Table VI we can see that the RCP mainly consists of $\Delta J=-1$ states, the LCP $\Delta J=+1$, and the $LP\|$ $\Delta J=0$. The factor for $LP\perp$ is given by $\frac{1}{2}(A^{+1}_{JJ'}+A^{-1}_{JJ'})$. In the $4d$ XAS there is little energy difference among the three ΔJ states because of small exchange integrals. Although the three ΔJ spectra are added differently according to the polarization of light, it does not strongly change the shape of spectrum but the intensity is changed. On the other hand, in the $5d$ XAS there is a large energy difference among three ΔJ spectra except for Cm which has a $L=0$ ground state, and the energy of their peaks always increases according to $\Delta J=+1,0,-1$, because the spin, and therefore the exchange energy is larger, on average, for the final states with larger J. This explains why the RCP spectra have a peak on the high-energy side and the LCP on the low-energy side The difference in the total intensity of MXD can also be understood from Table VI. The RCP has coefficients for all ΔJ states, but the LCP has only for $\Delta J=1$. Since the sum of these coefficients is larger for RCP, if the three spectra have almost the same intensity, the intensity for RCP becomes about 1.5 times larger than LCP. This is the case when the number of f electrons (n) is less than 7. When n is larger than 7, the intensity of $\Delta J=1$ states itself becomes smaller. This is because the J value of the ground state becomes large for $n>7$ and so the number of the $\Delta J=1$ final states becomes small. For $LP\|$, the $\Delta J=0$ states are mainly excited, and for $LP\perp$ linear combinations of the other two states are excited. This explains why the $LP\|$ spectra show one peak in the middle and the $LP\perp$ spectra show a peak on both sides.

TABLE VI. Typical values of the factor $A^m_{JJ'}(0)$.

	$m=+1$	$m=0$	$m=-1$
A^m_{JJ+1}	$\simeq 0$	$\simeq 0.2$	$\simeq 0.8$
A^m_{JJ}	$\simeq 0.2$	$\simeq 0.8$	0
A^m_{JJ-1}	1.0	0	0

V. CONCLUDING REMARKS

We calculated the magnetic dichroism in $4d$ and $5d$ XAS of actinides. This paper is intended to be a first approximation to the spectra of actinide ions in solids with the simplest model of free actinide ions, where all parameters except for broadening width Γ are determined by first principle Hartree-Fock calculations. It is to be mentioned that this ionic approach is only expected to be quantitatively correct for actinide elements heavier than Am, in which the actinide $5f$ electrons are well localized. In particular, most of U compounds, for which the first MXD experiments are expected in the near future, have been found to form itinerant $5f$ bands or mixed valence $5f$ states. Even for these materials we expect that our results are applicable qualitatively or semiquantitatively, because the MXD detects the local electronic character around a core hole, and especially in the final state of XAS the $5f$ electrons are more or less localized due to the local Coulomb interaction with the core hole. Therefore, the ionic approach is a reasonable one as a first approximation. However, the MXD is also sensitive to the orbital and spin states of $5f$ electrons in the initial state, and thus the study on the solid-state effects such as the crystal field, the hybridization, and the $5f$ band is necessary at the next step.

MXD of $4d$ XAS are not so remarkable as those of lanthanide $3d$ XAS, because the small exchange integrals between core and f orbits split the different ΔJ groups in the final state only slightly. Furthermore the large $5f$ spin-orbit interaction makes the branching ratio of $4d$ XAS for actinides much larger than that of $3d$ XAS for lanthanides. It is expected that the branching ratio is sensitive to solid-state effects such as the crystal field and the hybridization. The explicit study will be made in our future publication.

MXD of $5d$ XAS is expected to be large, like the lanthanide $4d$ XAS. The $LP\perp$ spectra typically have a double-peak structure, while the $LP\|$ spectra show a single peak. The RCP spectra are stronger than the LCP spectra, and the peak energy of RCP is higher than that of LCP. Since distinction between the prethreshold region and the giant absorption is unclear for the elements heavier than Np, we calculated the $5d$ XAS spectra by using a single spectral broadening Γ corresponding to the giant absorption region. A more careful treatment will be necessary for the spectra in the prethreshold region.

ACKNOWLEDGMENTS

We thank Dr. K. Okada for valuable discussion. This paper is partly supported by an International Joint Research Project from JSPS and by a Grant-in-Aid for Scientific Research from the Ministry of Education, Science and Culture in Japan. A part of this paper was prepared while one of the authors (A.K.) visited the University of Groningen, and he would like to thank Professor G. A. Sawatzky for hospitality.

---

*Present address: Institute for Solid State Physics, University of Tokyo, 7-22-1 Roppongi, Minato-ku, Tokyo 106, Japan.

[1]See, for instance, *Core-Level Spectroscopy in Condensed Systems,* edited by J. Kanamori and A. Kotani (Springer, Heidelberg, 1988).

[2]B. T. Thole, G. van der Laan, J. C. Fuggle, G. A. Sawatzkey, R. C. Karnatak, and J-M. Esteva, Phys. Rev. B **32**, 5107 (1985).

[3]J. Sugar, Phys. Rev. B **5**, 1785 (1972).

[4]B. T. Thole, G. van der Laan, and G. A. Sawatzky, Phys. Rev. Lett. **55**, 2086 (1985).

[5]G. van der Laan, B. T. Thole, G. A. Sawatzky, J. B. Goedkoop, J. C. Fuggle, J-M. Esteva, R. Karnatak, J. P. Remeika, and H. A. Dabkowska, Phys. Rev. B **34**, 6529 (1986).

[6]J. B. Goedkoop, B. T. Thole, G. van der Laan, G. A. Sawatzky, F. M. F. de Groot, and J. C. Fuggle, Phys. Rev. B **37**, 2086 (1988).

[7]J. B. Goedkoop, Ph.D. thesis, University of Nijmegen.

[8]G. Schütz, W. Wagner, W. Wilhelm, P. Kienle, R. Zeller, R. Frahm, and G. Materlik, Phys. Rev. Lett. **58**, 737 (1987).

[9]G. Schütz, M. Knuelle, R. Wienke, W. Wilhelm, W. Wagner, P. Kienle, and R. Frahm, Z. Phys. B **73**, 67 (1988).

[10]J. B. Goedkoop, J. C. Fuggle, B. T. Thole, G. van der Laan, and G. A. Sawatzky, Nucl. Instrum. Methods A **273**, 429 (1988).

[11]T. Jo and S. Imada, J. Phys. Soc. Jpn. **59**, 2312 (1990).

[12]S. Imada and T. Jo, J. Phys. Soc. Jpn. **59**, 3358 (1990).

[13]B. W. Veal, D. J. Lam, H. Diamond, and H. R. Hoedstra, Phys. Rev. B **15**, 2929 (1977).

[14]G. Kalkowski, G. Kaindl, W. D. Brewer, and W. Krone, Phys. Rev. B **35**, 2667 (1987).

[15]M. Cukier, P. Dhez, B. Gauthé, P. Jaeglé, Cl. Wehenkel, and F. Combet Farnoux, J. Phys. **39**, L315 (1978).

[16]C. G. Olsen and D. W. Lynch, J. Opt. Soc. Am. **72**, 88 (1982).

[17]R. D. Cowan, *The Theory of Atomic Structures and Spectra* (University of California Press, Berkeley, 1981).

[18]B. T. Thole and G. van der Laan, Phys. Rev. A **38**, 1943 (1988).

[19]Our definition of $A^{m}_{JJ'}(\Theta)$ is different from that in Ref. 6 by a factor of $2J+1$.